RSC Advances

PAPER

View Article Online
View Journal | View Issue

Cite this: *RSC Adv.*, 2017, **7**, 39686

A DFT analysis on the radical scavenging activity of oxygenated terpenoids present in the extract of the buds of *Cleistocalyx operculatus*†

Thi Chinh Ngo,[a] Duy Quang Dao,*[a] Minh Thong Nguyen[b] and Pham Cam Nam[c]

The antioxidant capacity of twenty-one oxygenated monoterpene and oxygenated desquiterpene compounds in the extract from *Cleistocalyx operculatus* has been computationally evaluated. Calculated by (RO)B3LYP/6-311++G(2df,2p)//B3LYP/6-311G(d,p) model chemistries, the thermochemical parameters, namely BDE, IE, PDE, PA and ETE in the gas phase, water and ethanol were determined. In addition, quantum descriptors, which allow the evaluation of the reactivity and stability of the resulting radicals like chemical potential (μ), hardness (η) and global electrophilicity (ω) were also computed. Potential energy surfaces of the reactions between $CH_3OO^{\bullet}$ and $HO^{\bullet}$ radicals with falcarinol and α-vetivone, two typical and potential antioxidant molecules, were established to give more insight into the antioxidant mechanism. The obtained results underline falcarinol as the most effective antioxidant with the lowest BDE of 66.5 kcal mol^{-1} and PA of 341.3 kcal mol^{-1} in the gas phase. Among the reactions on falcarinol, the H-abstraction at C3–H position by both $CH_3OO^{\bullet}$ and $HO^{\bullet}$ radicals are favorable with the energy barriers of −18.7 and −54.7 kcal mol^{-1}, respectively. Moreover, NBO analysis helps to clarify the mechanism of antioxidant action which shows that the third lone pair of electrons on O1-atom of $CH_3OO^{\bullet}$ radical is donated to an unoccupied σ^*-antibonding orbital on C3–H, and on the C4≡C5, C6≡C7 triple bonds. Similarly, attack of $CH_3OO^{\bullet}$ and $HO^{\bullet}$ radicals on α-vetivone demonstrates that H-abstraction reactions are also more feasible than the addition ones with ΔH values of −7.3 and −41.9 kcal mol^{-1}, respectively. For all considered reactions, the antioxidant molecules preferentially interact with $HO^{\bullet}$ radical.

Received 28th April 2017
Accepted 8th August 2017

DOI: 10.1039/c7ra04798c

rsc.li/rsc-advances

1. Introduction

Essential oils, aromatic and volatile liquids, are principally extracted from various parts (flowers, seed, leaves, fruits…) of numerous natural plants (tea, pepper, ginger, thyme…).[1–5] They have been attractive subjects for applications in industry (for flavoring food, perfumes, cosmetics, *etc.*) as well as in pharmaceutical and medicinal domains.[6–9] The essential oils are generally rich in terpenoid compounds, mainly mono-, sesqui- and desquiterpenes which are hydrocarbon or oxygenated compounds.[7,10] These interesting oils have already been well-known in a number of applications such as antimicrobial, anticancer, antifungal, antiviral and especially antioxidant.[4,11–17] For example, the results obtained by 2,2-diphenyl-1-picrylhydrazyl (DPPH) and nitric oxide scavenging assays clearly indicate that the essential oils isolated from fresh rhizomes of garlic (*Allium Sativum*) of the family Alliaceae are effective in scavenging free radicals, so they potentially have a powerful antioxidant role.[16] In the work of Bozin *et al.*[17] the antioxidant activities of the essential oils of *Lamiaceae* species including *Ocimum basilicum* L., *Origanum vulgare* L., and *Thymus vulgaris* L. were evaluated to play a role in a free radical scavenging capacity (RSC), together with effects on lipid peroxidation (LP). The investigated essential oils exhibit high RSC against DPPH radical and inhibit a very strong lipid peroxidation induced by both Fe^{2+}/ascorbate and Fe^{2+}/H_2O_2. Otherwise, the antioxidant properties of the essential oils extracted from *Cleistocalyx operculatus* are also well-known.[18] A variety of organic compounds including monoterpenes, oxygenated monoterpenes, sesquiterpenes, oxygenated desquiterpenes and diterpenes were experimentally identified and measured antioxidant properties on the basis of the scavenging activities of the stable 2,2-diphenyl-1-picrylhydrazyl (DPPH) free radical.[18] Additionally, the antioxidant mechanism of these three hydrocarbon terpenoid classes including monoterpenes, sesquiterpenes and diterpenes has theoretically been clarified in our previous study.[19] Some of them (α-terpinene, γ-terpinene,

[a]*Institute of Research and Development, Duy Tan University, 03 Quang Trung, Danang, Vietnam. E-mail: daoduyquang@gmail.com*

[b]*The University of Danang, Campus in Kon Tum, 704 Phan Dinh Phung, Kon Tum, Vietnam*

[c]*Department of Chemistry, The University of Da Nang – University of Science and Technology, 54 Nguyen Luong Bang, Lien Chieu, Danang, Vietnam*

† Electronic supplementary information (ESI) available. See DOI: 10.1039/c7ra04798c

cembrene and abieta-7,13-diene) have promising antioxidant properties. The ability to scavenge reactive oxygen species (ROS), one of essential requirements for antioxidant role, of selected α-terpinene was consequently ascertained *via* its interaction with hydroperoxyl radicals (HOO˙).[19]

Moreover, several experimental works in literature[20–23] have been discussed that oxygenated compounds available in *Cleistocalyx operculatus* like falcarinol, α-vetivone and so on, represent also as potential health promoting compounds. In fact, falcarinol, one of aliphatic C17-polyacetylenes which can be found in common food plants such as carrot, celeriac, parsnip and parsley, shows a number of interesting bioactivities such as antibacterial, antimycobacterial, and antifungal activity, anti-inflammatory, anti-platelet-aggregatory, as well as neurotogenic and serotonergic effects.[20,21,23] α-vetivone, one of the most important constituents isolated and identified from crude vetiver (*Vetiveria zizanioides* L.) oil, has strong antioxidant activities *via* DPPH free radical scavenging assay and the Fe^{2+}-metal chelating assay.[24]

Hence, in this paper, our interest is set on two classes namely oxygenated monoterpenes and oxygenated desquiterpenes, whose structures contain oxygen atom. For more detail, the insight into the theoretical mechanism of antioxidant activity of these compounds will be clarified *via* three mechanisms of antioxidant action including hydrogen atom transfer (HAT), single electron transfer followed by-proton transfer (SET-PT) and sequential proton loss electron transfer (SPLET). First and foremost, the calculations of various thermochemical parameters including bond dissociation enthalpy (BDE), proton affinity (PA), electron transfer enthalpy (ETE) and ionization energy (IE)

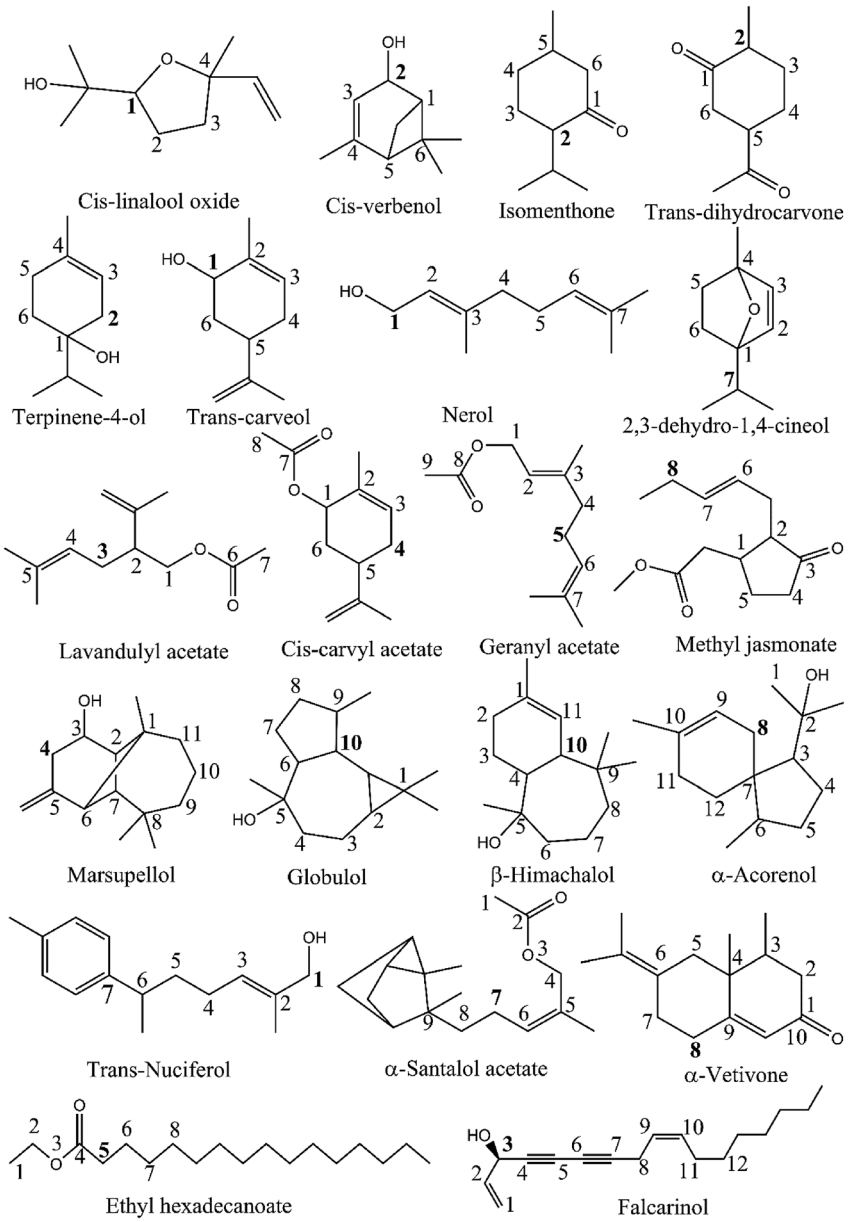

Fig. 1 Chemical structure of 21 studied compounds.

are performed using the density functional theory (DFT) method at the model chemistry of (RO)B3LYP/6-311++G(2df,2p)//B3LYP/6-311G(d,p) in the gas phase, ethanol and water which is a typical polar solvent ($\varepsilon = 78.36$).

In the next step, the global descriptive parameters including chemical potential (μ), chemical hardness (η) and global electrophilicity (ω) of neutral compounds will be calculated to elucidate their reactivity and stability. Finally, potential energy surface (PES) of all possible addition reactions as well as H-abstraction ones between the most potential antioxidant compounds with $CH_3OO^{\bullet}$ and $HO^{\bullet}$ radical will be established to give more insights into free radical scavenging mechanism. In parallel, singly-occupied molecular orbital (SOMO), atomic spin density (ASP) and natural bond orbital (NBO) analysis of the optimized transition states will also be taken into account in order to explain clearly the mechanism of reactions.

2. Computational method

All calculations were performed using the Gaussian 09 software.[25] The geometry optimization and the vibrational frequency calculation of each compound and the corresponding radical, cationic radical and anion were primarily performed at the B3LYP/6-311G(d,p) level of theory. Their single point electronic energies were then calculated at the restricted-open shell (RO)B3LYP/6-311++G(2df,2p) level of theory. Generally, three common mechanisms of antioxidant action leading the same final products have been proposed and widely accepted as follows:[19,26]

• Hydrogen atom transfer (HAT):

$$R\text{–}H \rightarrow R^{\bullet} + H^{\bullet}\ (BDE)$$

• Single electron transfer followed by proton transfer (SET-PT)

$$R\text{–}H \rightarrow RH^{+\bullet} + e^{-}\ (IE)$$

$$RH^{+\bullet} \rightarrow R^{\bullet} + H^{+}\ (PDE)$$

• Sequential proton loss electron transfer (SPLET)

$$R\text{–}H \rightarrow R^{-} + H^{+}\ (PA)$$

$$R^{-} \rightarrow R^{\bullet} + e^{-}\ (ETE)$$

The reaction enthalpies of an antioxidant in gas phase at 298.15 K and 1 atm are calculated as follows:

$$BDE = H(R^{\bullet}) + H(H^{\bullet}) - H(R\text{–}H) \quad (1)$$

$$IE = H(RH^{\bullet+}) + H(e^{-}) - H(R\text{–}H) \quad (2)$$

$$PDE = H(R^{\bullet}) + H(H^{+}) - H(RH^{\bullet+}) \quad (3)$$

$$PA = H(R^{-}) + H(H^{+}) - H(R\text{–}H) \quad (4)$$

$$ETE = H(R^{\bullet}) + H(e^{-}) - H(R^{-}) \quad (5)$$

Table 1 The C–H bond dissociation enthalpy (BDE) in different media and PDEs in the gas phase of studied compounds using (RO)B3LYP/6-311++G (2df,2p)//B3LYP/6-311G(d,p) model chemistries

			BDEs (kcal mol^{-1})			PDEs (kcal mol^{-1})
	Compounds	Bonds	Gas phase	Water	Ethanol	Gas phase
Oxygenated monoterpenes	*cis*-Linalool oxide	C1–H	91.9	93.2	92.5	217.9
	cis-Verbenol	C2–H	78.5	80.2	79.7	205.6
	Isomenthone	C2–H	81.0	81.9	81.3	199.1
	trans-Dihydrocarvone	C2–H	84.8	85.7	85.1	201.6
	Terpinen-4-ol	C2–H	83.5	84.9	84.2	206.0
	trans-Carveol	C1–H	76.9	78.9	78.2	202.7
	Nerol	C1–H	79.2	81.0	80.4	213.8
	2,3-Dehydro-1,4-cineol	C7–H	95.2	96.8	96.1	212.1
	Lavandulyl acetate	C3–H	82.7	83.7	83.0	211.2
	cis-Carvyl acetate	C4–H	83.6	85.1	84.5	209.8
	Geranyl acetate	C5–H	83.1	84.3	83.7	217.5
	Methyl jasmonate	C8–H	83.3	84.8	84.1	206.4
Oxygenated desquiterpene	Marsupellol	C4–H	82.6	84.4	83.7	213.3
	Globulol	C10–H	92.8	94.2	93.6	234.4
	β-Himachalol	C10–H	82.3	84.0	83.3	217.0
	α-Acorenol	C8–H	81.2	82.8	82.1	216.6
	trans-Nuciferol	C1–H	82.4	84.1	83.5	215.5
	α-Santalol acetate	C7–H	82.2	83.6	83.0	218.7
	α-Vetivone	C8–H	78.1	79.2	78.6	210.0
	Ethyl hexadecanoate	C5–H	92.1	93.6	92.9	206.8
	Falcarinol	C3–H	66.5	69.3	67.9	194.4

Table 2 Vertical ionization energy (IE), electron affinity (EA), chemical potential (μ), chemical hardness (η) and global electrophilicity (ω) calculated at B3LYP/6-311++G(2df,2p)//B3LYP/6-311G(d,p) model chemistries (all parameters are in eV)

Compounds	IE	EA	μ	η	ω
cis-Linalool oxide	8.76	−0.42	−4.17	4.59	1.89
cis-Verbenol	8.40	−0.44	−3.98	4.42	1.79
Isomenthone	8.69	−0.38	−4.15	4.53	1.91
trans-Dihydrocarvone	8.69	−0.25	−4.22	4.47	1.99
Terpinen-4-ol	8.65	−0.42	−4.12	4.54	1.87
trans-Carveol	8.52	−0.39	−4.07	4.45	1.86
Nerol	8.13	−0.51	−3.81	4.32	1.68
2,3-Dehydro-1,4-cineol	8.95	−0.50	−4.23	4.72	1.89
Lavandulyl acetate	8.27	−0.49	−3.89	4.38	1.73
cis-Carvyl acetate	8.47	−0.39	−4.04	4.43	1.84
Geranyl acetate	8.15	−0.45	−3.85	4.30	1.72
Methyl jasmonate	8.42	−0.29	−4.06	4.36	1.90
Marsupellol	8.49	−0.55	−3.97	4.52	1.75
Globulol	8.14	−0.39	−3.88	4.27	1.76
β-Himachalol	8.21	−0.38	−3.92	4.29	1.79
α-Acorenol	8.09	−0.67	−3.71	4.38	1.57
trans-Nuciferol	8.02	−0.35	−3.83	4.19	1.76
α-Santalol acetate	8.27	−0.34	−3.97	4.31	1.83
α-Vetivone	8.06	0.02	−4.04	4.02	2.03
Ethyl hexadecanoate	9.09	−0.32	−4.38	4.71	2.04
Falcarinol	8.35	−0.27	−4.04	4.31	1.89

where H is the total enthalpy of the studied species at the temperature of 298.15 K and usually estimated from the expression below: $H = E_0$ + ZPE + H_{trans} + H_{rot} + H_{vib} + RT.

The H_{trans}, H_{rot}, and H_{vib} are the translational, rotational and vibrational contributions to the enthalpy, respectively. E_0 is the total energy at 0 K and ZPE is the zero-point vibrational energy. The enthalpies of H-atom ($H^{\bullet}$), proton (H^{+}), and electron (e^{-}) are taken from literature.[27] Vibrational frequencies obtained at the B3LYP/6-311G(d,p) level of theory were scaled by a factor of 0.9669.[28] The calculation in solvents was based on integral equation formalism of polarizable continuum model (IEF-PCM) at the same level of theory as in the gas phase.[29,30] The influence of water and ethanol on the thermodynamic properties was discussed.

To evaluate reactivity and stability of the studied compounds we used global theoretical descriptors that were calculated at B3LYP/6-311++G(2df,2p)//B3LYP/6-311G(d,p). Finite differences method proposed by Pearson and Parr is used to approximately determine chemical potential (μ),[31,32] chemical hardness (η)[33] and global electrophilicity (ω)[34] on the basis of vertical electron affinity (EA) and ionization energy (IE) of chemical species as follows:

$$\mu = -\frac{1}{2}(\mathrm{IE} + \mathrm{EA})$$

$$\eta = \frac{1}{2}(\mathrm{IE} - \mathrm{EA})$$

$$\omega = \frac{\mu^2}{2\eta}$$

Potential energy surface (PES) of the most potential antioxidant compound was also established. The calculation of geometric optimization and vibrational frequencies respectively of transition states, of reactant complexes and of product

Table 3 Proton affinity (PA) and electron transfer enthalpy (ETE) of studied compounds using (RO)B3LYP/6-311++G(2df,2p)//B3LYP/6-311G(d,p) model chemistries

		PA (kcal mol^{-1})			ETE (kcal mol^{-1})		
Compounds	Bonds	Gas phase	Water	Ethanol	Gas phase	Water	Ethanol
cis-Linalool oxide	O–H	369.1	57.2	74.9	51.0	70.7	89.2
cis-Verbenol	O–H	369.9	54.1	71.9	46.3	69.7	88.2
Isomenthone	C2–H	363.2	50.5	67.9	32.3	52.2	71.1
trans-Dihydrocarvone	C2–H	356.5	50.7	68.1	43.9	57.9	76.4
Terpinen-4-ol	O–H	369.6	56.2	74.0	47.5	68.4	86.9
trans-Carveol	O–H	370.3	53.6	71.4	45.9	70.8	89.2
Nerol	C4–H	377.3	70.0	87.1	23.7	38.2	57.4
2,3-Dehydro-1,4-cineol	C6–H	400.7	90.1	107.7	13.6	31.9	50.6
Lavandulyl acetate	C7–H	369.2	56.4	74.0	43.6	64.2	82.8
cis-Carvyl acetate	C8–H	367.6	56.1	73.6	45.1	64.5	83.2
Geranyl acetate	C9–H	370.0	56.7	74.3	42.7	63.9	82.5
Methyl jasmonate	C2–H	356.2	49.7	67.1	44.5	58.1	77.0
Marsupellol	O–H	366.3	53.7	71.4	48.6	69.2	87.7
Globulol	O–H	365.2	55.9	73.5	49.2	66.2	84.8
β-Himachalol	O–H	367.2	56.8	74.4	48.3	66.5	85.1
α-Acorenol	O–H	366.2	55.9	73.5	49.1	67.1	85.7
trans-Nuciferol	O–H	372.7	53.1	70.9	44.4	72.1	90.5
α-Santalol acetate	C1–H	369.0	56.9	74.5	43.8	63.7	82.3
α-Vetivone	C8–H	351.0	44.1	61.4	41.7	55.9	74.8
Ethyl hexadecanoate	C5–H	369.1	58.7	76.2	37.6	55.8	74.4
Falcarinol	C8–H	341.3	41.6	58.7	46.3	51.8	70.9

complexes were investigated at B3LYP/6-311G(d,p) level of theory for all possible adduction reactions as well as H-abstraction ones.

3. Results and discussion

3.1. Thermochemical parameters characterizing antioxidant capacity

3.1.1. Antioxidant capacity *via* hydrogen atom transfer – bond dissociation enthalpy. The chemical structures of oxygenated mono- and desquiterpenes, which generally contain oxygen atom and unsaturated bonds, found in the buds of *Cleistocalyx operculatus* are showed in Fig. 1. In order to evaluate the activity of an antioxidant *via* hydrogen donating mechanism, the C–H and O–H homolytic bond dissociation enthalpies (BDEs) which relate to the abilities of donating hydrogen atom and of forming radical species, are taken into account. The lowest BDE is defined for the relevant position of C–H/O–H where the easiest abstraction hydrogen for free radical scavenging reaction can take place. Hence, BDE is an appropriate descriptor of the antioxidant activity.

As observed in the previous study,[19] the C–H bonds neighboring C=C double bonds are detected to be the easiest breaking bonds in comparing to other ones due to the reason that the electron-withdrawing inductive effect ($-I$) of the π-bond induces an electron-releasing phenomenon from the carbon atoms, and consequently increases the polarization of the C–H bonds. Therefore, these bonds were reasonably

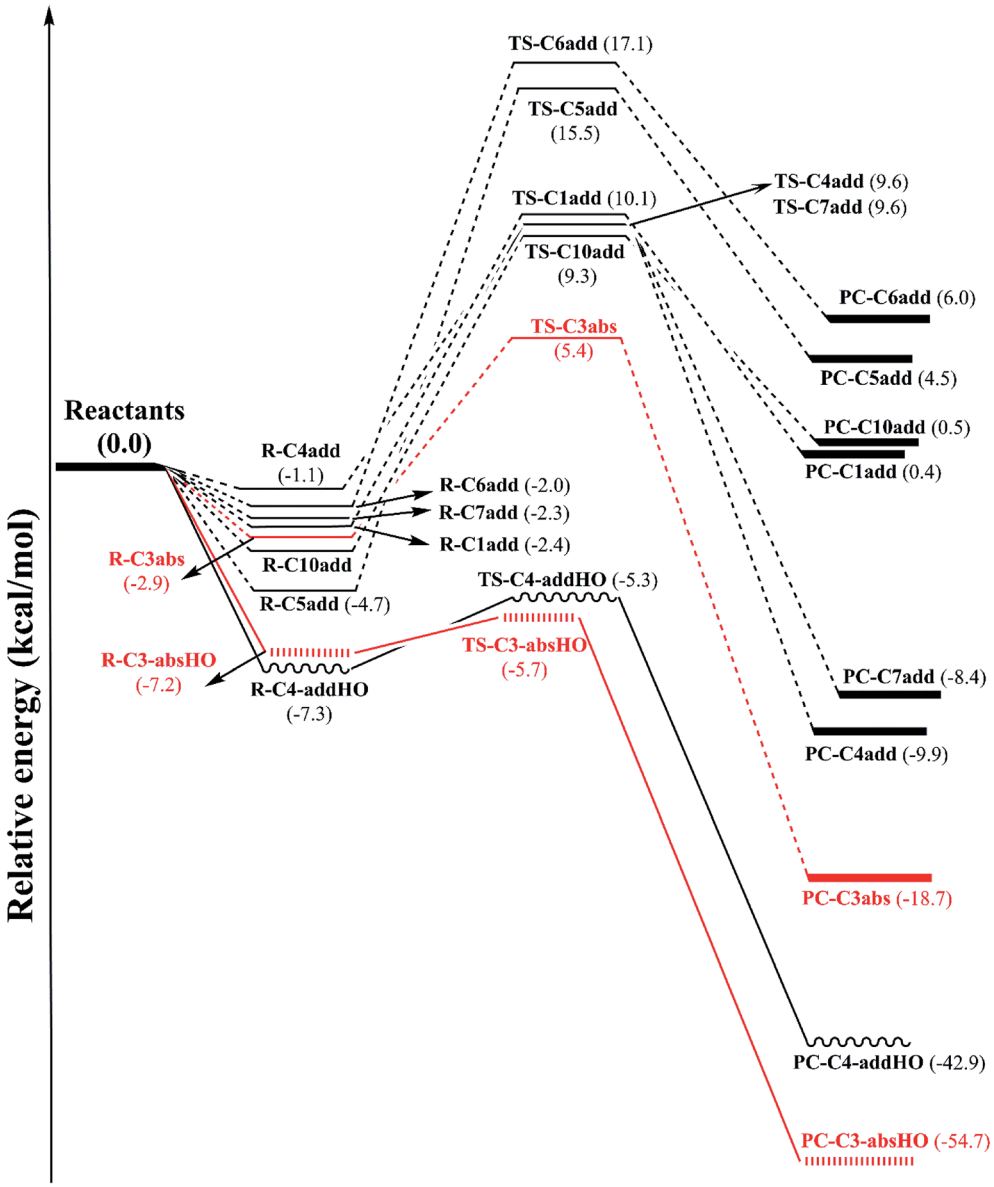

Fig. 2 Potential energy surface (PES) at B3LYP/6-311G (d,p) level of theory of H-abstraction reaction at easiest breaking bond and addition reaction at unsaturated bond positions between $CH_3OO^{\bullet}$ and $HO^{\bullet}$ radicals and falcarinol. (The abbreviation containing HO indicates for the reactions with $HO^{\bullet}$, the rest is of the ones with $CH_3OO^{\bullet}$).

selected to compute their strength at the higher level of theory of (RO)B3LYP/6-311++G(2df,2p)//B3LYP/6-311G(d,p). The BDEs of weakest bonds are present in Table 1. Cartesian coordinates and enthalpies of all parent molecules and resulted radicals, anions optimized at B3LYP/6-311G(d,p) level of theory in the gas phase, water and ethanol are presented in Table S1 ESI.†

Table 1 demonstrates that the BDEs (C–H) of studied compounds vary from 66.5 to 95.2 kcal mol^{-1}. The lowest BDE (C–H) of 66.5 kcal mol^{-1} is indicated for falcarinol which contains two conjugated triple bonds and two double bonds in its structure. It means that the number of C=C double and C≡C triple bonds present in molecular system has a significant effect on the BDEs. In fact, the lower BDE (C–H) (*i.e.* 78.1 kcal mol^{-1}) of α-vetivone compared to the others is also related to the presence of two conjugated π-bonds nearby that C position (as can be seen in Fig. 1). As the number of conjugated double/triple bonds increases, the electrons associated with conjugated systems have more space to delocalize and require less energy to change states. This results are coherent with the previous study.[19]

In addition, the presence of OH group also contributes to the changing of the BDE values. In fact, the C–H bonds located nearby both OH group and unsaturated bonds possess lower BDE values compared to other ones. For example, the BDEs of *cis*-verbenol, *trans*-carveol and nerol are, in principle, lower than 80 kcal mol^{-1}, being 79.2, 76.9 and 78.6 kcal mol^{-1}, respectively.

Regarding the effect of solvents on BDEs, there is occurred no remarkable difference between the results computed in the gas phase and two solvents (water and ethanol). For example, the BDEs calculated in the gas phase, water and ethanol of falcarinol are 66.5, 69.3 and 67.9 kcal mol^{-1}, respectively. Similarly, the calculated values in these three phases for *trans*-carveol are 76.9, 78.9 and 78.2 kcal mol^{-1}, respectively. This leads to conclude that hydrogen atom transfer is favored in nonpolar environments.

3.1.2. Antioxidant capacity *via* electron transfer – ionization energy (IE). Ionization energy which characterizes for electron transfer ability, equally serves as a general parameter for evaluating radical scavenging potency of antioxidants *via* SET-PT mechanism. The higher the IE is, the more difficult an electron can be removed. The results show the lowest IEs of 8.02, 8.06 and 8.09 eV corresponding to *trans*-nuciferol, α-vetivone and α-acorenol, while the highest one of 9.09 eV assigning to ethyl hexadecanoate (Table 2). It means that electron removal from those three molecules is more favorable.

In parallel with IE values, the global reactivity descriptors including chemical potential (μ), chemical hardness (η) and global electrophilicity (ω) calculated based on IE and EA values give more information about the tendency of selectivity and chemical reactivity of parent compounds and their radical formed *via* easiest C–H breaking bonds (data present in Table 2). For example, chemical hardness (η), which is defined as the resistance of cloud polarization or deformation of chemical species, is used to predict the reactivity of molecules. The lowest value of hardness means the highest reactivity. Regarding the hardness values present in Table 2, α-vetivone is seen to be the most reactive in comparison with the hardness of the other compounds noted 4.02 eV. In terms of global electrophilicity (ω) representing the capacity of a system to acquire an electron, a higher ω value demonstrates the more reactive molecule. Among these studied compounds, α-vetivone and ethyl hexadecanoate show as the most reactive ones with the ω value of 2.03 and 2.04 eV, respectively.

The following step of electron transfer *via* SET-PT mechanism is proton transfer process from C–H group of the formed cationic radical that is characterized by proton dissociation enthalpy (PDE). The PDE values for deprotonation of all cationic

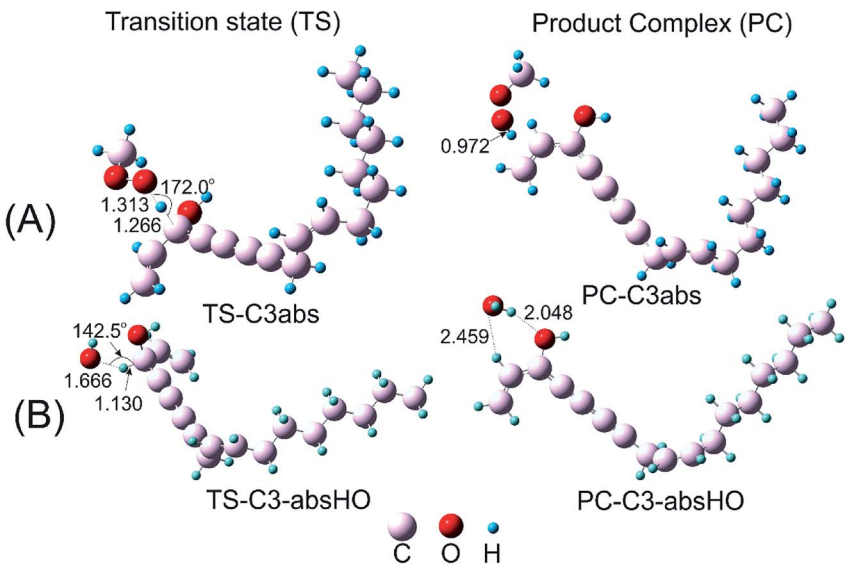

Fig. 3 Optimized geometries of transition state (TS) and product complex (PC) species for the H-atom abstraction between falcarinol and (A) $CH_3OO^{\bullet}$ and (B) $HO^{\bullet}$ radical at the B3LYP/6-311G(d,p) level of theory, (distances are given in angstroms).

radical species are displayed in Table 1 and indicates that the easiest deprotonation generally found at the C–H position with the lowest BDE. As a result, the lowest PDEs are 194.4 and 199.1 kcal mol^{-1} corresponding to the cationic radical formed from falcarinol and isomenthone, respectively. It is noted that falcarinol demonstrates both the easiest homolytic and heterolytic H-dissociation.

3.1.3. Antioxidant capacity *via* sequential proton loss electron transfer (SPLET) – proton affinity (PA) and electron transfer enthalpy (ETE). Proton affinity (PA) and electron transfer enthalpy (ETE) are two physicochemical parameters used to examine antioxidant activity *via* SPLET mechanism. In principle, from mother compounds, a SPLET mechanism occurs *via* two successive steps which are a proton loss process characterized by PA value, and then an electron transfer symbolized by ETE value. The lower the PA is, the higher the antioxidant activity can be marked. The PAs of all possible bonds breaking were firstly calculated by the semi-empirical PM6 method to find out the easiest deprotonation positions. The PAs of relevant bonds were then computed at higher (RO)

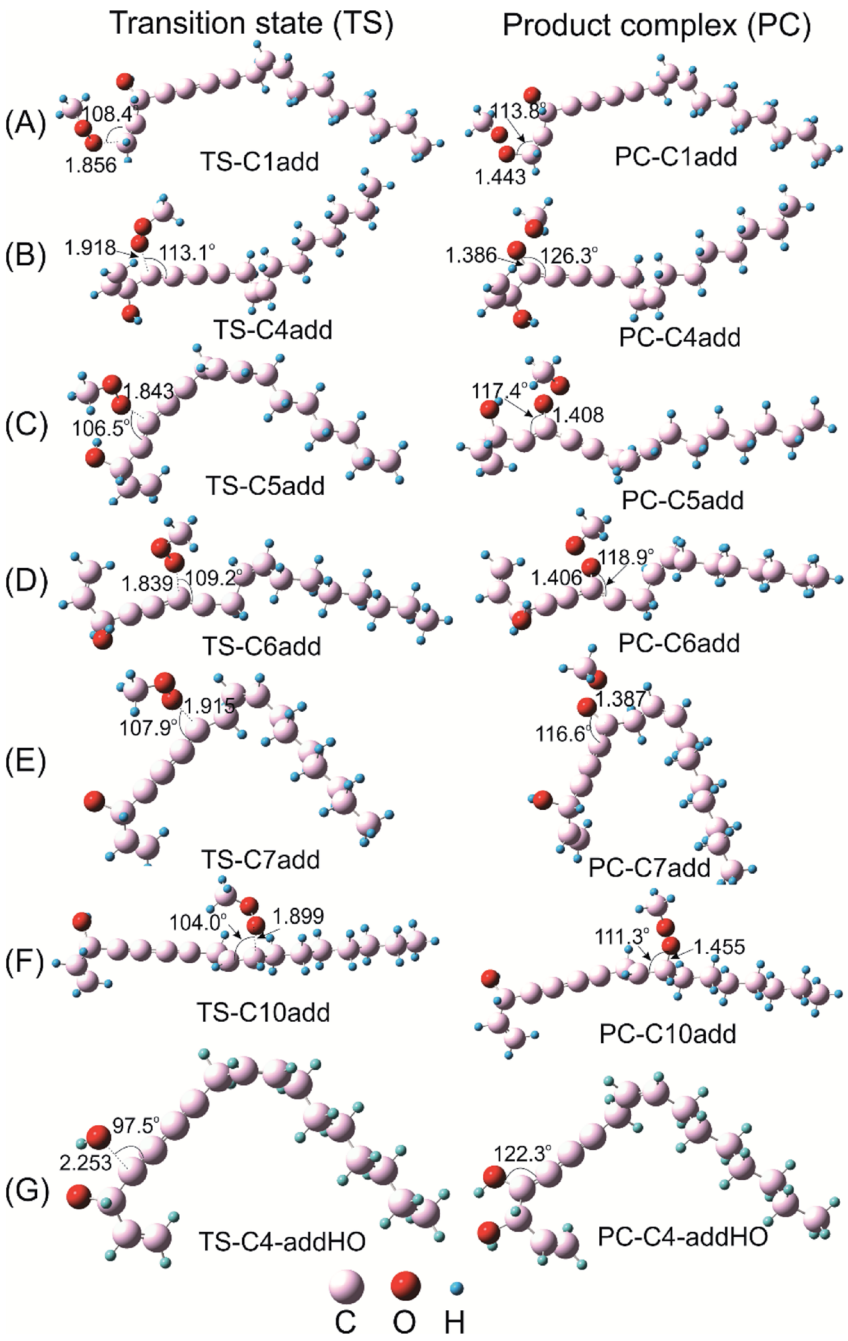

Fig. 4 Optimized geometries of transition state (TS) and product complex (PC) of addition reaction at unsaturated bond positions between falcarinol and $CH_3OO^{\bullet}$ radical (A–F) and $HO^{\bullet}$ radical (G). All calculations were performed at B3LYP/6-311G(d,p) level of theory.

Table 4 Reaction enthalpies (ΔH) and Gibbs energies (ΔG) (in kcal mol^{-1}) for the H-atom abstraction at easiest H-breaking bond and the addition reactions between falcarinol (FALC) and α-vetivone (VET) and $CH_3OO^\bullet$ and $HO^\bullet$ radicals

Reactions	ΔH, kcal mol^{-1}	ΔG, kcal mol^{-1}
FALC–C3H + $CH_3OO^\bullet$	−18.7	−10.0
FALC–C10 + $CH_3OO^\bullet$	0.5	12.6
FALC–C7 + $CH_3OO^\bullet$	−8.4	3.1
FALC–C6 + $CH_3OO^\bullet$	6.0	18.0
FALC–C5 + $CH_3OO^\bullet$	4.5	16.6
FALC–C4 + $CH_3OO^\bullet$	−9.9	1.7
FALC–C1 + $CH_3OO^\bullet$	0.4	12.4
FALC–C3H + $HO^\bullet$	−54.7	−47.1
FALC–C4 + $HO^\bullet$	−42.9	−32.2
VET–C8H + $CH_3OO^\bullet$	−7.3	1.5
VET–C8H + $HO^\bullet$	−41.9	−36.2
VET–C9 + $CH_3OO^\bullet$	4.8	18.0
VET–C9 + $HO^\bullet$	−25.3	−14.3

B3LYP/6-311++G(2df,2p)//B3LYP/6-311G(d,p) level of theory. The obtained results are given in Table 3.

It is generally observed that heterolytic cleavage is favored at O–H and C–H position located nearby C=C double bonds. The best antioxidant based on SPLET mechanism is falcarinol with the PAs computed in the gas phase of 341.3 kcal mol^{-1}. In the meantime, when calculating in polar solvents, one observed a dramatic decrease in PAs by comparison with the values measured in the gas phase. In fact, the PA of *cis*-linalool oxide in the gas phase is 369.1 kcal mol^{-1} while its values in water and ethanol are 57.2 and 74.9 kcal mol^{-1}, respectively. Similarly, the PAs of falcarinol are 341.3, 41.6 and 58.7 kcal mol^{-1} assigned to the calculation in the gas phase, water and ethanol, respectively. This observation can be explained by the higher solvation enthalpy of proton in water and ethanol compared to that in the gas phase, and also it is in a good agreement with the results obtained in previous studies.[19,26,35] Indeed, Thong *et al.* showed the PAs of α-mangostin are 326.0 and 23.6 kcal mol^{-1} at B3LYP/6-31+G(d,p) level of theory in the gas phase and water, respectively.[26] The PAs obtained for a hydroxylchalcone by Wang and coworkers are 354.6 kcal mol^{-1} in the gas phase and 58.5 kcal mol^{-1} in water at B3LYP/6-311++G(2d,2p) level of theory.[35] In conclusion, the deprotonation process of an antioxidant is favored in polar environments.

Regarding the electron transfer enthalpy (ETE) which represents the electron donating ability of anion formed in the first step of the SPLET mechanism, one observed that the ETEs in the gas phase (as seen in Table 3) are relatively lower than IEs (data in Table 2). For example, ETE of *cis*-linalool oxide in the gas phase is 51.0 kcal mol^{-1} while IE is 206.1 kcal mol^{-1} (or 8.94 eV). It means that the electron transfer from anionic form is more favorable than that from neutral one. This is coherent with the results reported in previous studies.[19,26,36,37]

Among studied compounds, falcarinol seems to be the most efficient antioxidant molecule *via* both HAT and SPLET mechanisms. And α-vetivone is also a promising antioxidant compound. Therefore, in the following section, falcarinol and α-vetivone are considered as a model molecule to investigate their interaction with $CH_3OO^\bullet$ and $HO^\bullet$ radicals which are chosen as representative free radical model for $ROO^\bullet$ and $RO^\bullet$ one.

3.2. Interaction of typical free radicals with potential antioxidant molecules

Falcarinol which contains two conjugated triple bonds and two double bonds shows as the easiest H-donating compound with the BDE (C3–H) in the gas phase of 66.5 kcal mol^{-1}. It can play a role in scavenging free radical *via* either H-abstraction at C3–H or addition at the unsaturated bonds. Reactions between falcarinol and $CH_3OO^\bullet$ radical will be discussed in turn the H-abstraction channel at C3–H and the addition channel at C1=C2, C9=C10 double and C4≡C5, C6≡C7 triple bonds (see Fig. 1). The potential energy surfaces (PES) of these reactions are established and displayed in Fig. 2. All optimized structures and the corresponding energies of the species related to the mentioned reaction were computed at B3LYP/6-311G(d,p) level. IRC plots for all transition states related to reactions of $CH_3OO^\bullet$ and $HO^\bullet$ radicals with falcarinol are presented in Fig. S2 of ESI.†

3.2.1. Hydrogen abstraction reaction by free radical at the easiest H-donating position. H-abstraction reaction by $CH_3OO^\bullet$ and $HO^\bullet$ radical at C3–H of falcarinol (FALC–H) (see Fig. 1) is demonstrated as below:

$$CH_3OO^\bullet/HO^\bullet + FALC\text{–}H \rightarrow FALC^\bullet + CH_3OOH/H_2O$$

PES of H-abstraction and radical addition to unsaturated bonds reactions of falcarinol with $CH_3OO^\bullet$ and $HO^\bullet$ radical is displayed in Fig. 2. All the optimized geometries of transition state (TS) and product complex (PC) are shown in Fig. 3 and 4. TS structure of H-abstraction reaction between falcarinol with DPPH radical is also presented in Fig. S4 of ESI.†

The H-atom transfer from C3–H bond of falcarinol to the $CH_3OO^\bullet$ radical is occurred in initiation step and demonstrated as an important one in interrupting the chain reactions.[38] In the H-abstraction reaction, the $CH_3OO^\bullet$ radical and falcarinol reactants can form a hydrogen-bonded reactant complex (R–C3) at energy lying below the separated reactants by −2.3 kcal mol^{-1}. In this state, a hydrogen bond is generated between O-atom of $CH_3OO^\bullet$ and H-atom at C3–H of falcarinol, and $CH_3OO\cdots H$–C3 distance is 2.447 Å (as seen in Fig. 3). Then, the H-atom of falcarinol tends to form a chemical bond with the O-atom of the radical *via* a transition state (TS-C3abs) lying at 5.4 kcal mol^{-1} above the reactants where the $CH_3OO\cdots H$–C3 distance is shorter. The H-atom is situated in the middle of O and C3 atoms and the $CH_3OO\cdots H$ and H–C3 distance are 1.313 and 1.266 Å, respectively. The C3–H–O angle is relatively bent, being 172° (Fig. 3). After passing these states, the reaction pathway reaches the product complex (PC-C3abs) containing $FALC^\bullet$ radical and CH_3OOH at −18.7 kcal mol^{-1} below the reactants, in which a covalent chemical bond of 0.972 Å is formed between O and H-atom. It is worth noting that the H-abstraction reaction at the easiest breaking bond requires lower reaction barriers compared to the addition ones (see Fig. 2). In addition, the Gibbs energy (ΔG) presented in Table 4

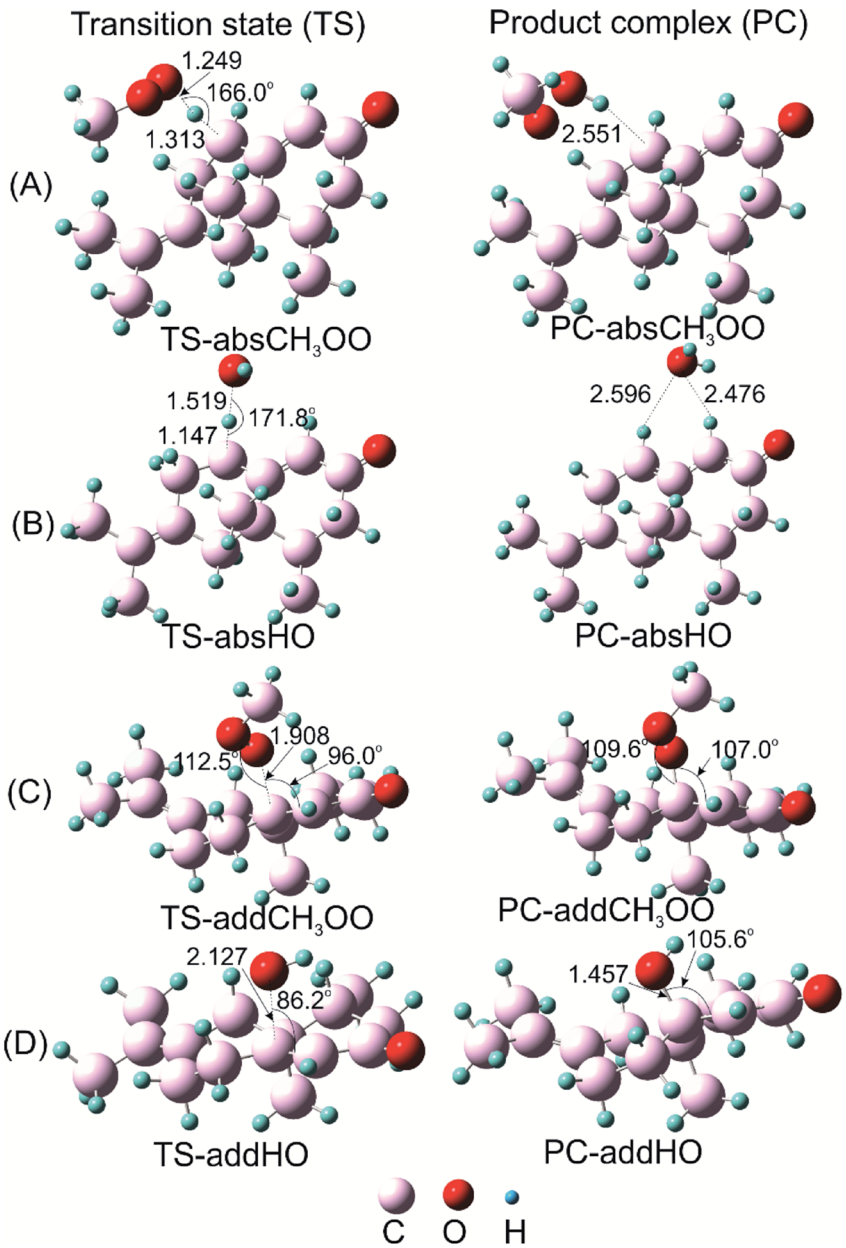

Fig. 5 Optimized geometries of transition states (TS) and product complexes (PC) of H-atom abstraction reactions of α-vetivone with (A) $CH_3OO^{\bullet}$ radical, (B) $HO^{\bullet}$ radical at C8–H position; and of addition reactions to double bonds for (C) $CH_3OO^{\bullet}$ radical and (D) $HO^{\bullet}$ radical at C9 position.

shows that the H-abstraction reaction by $CH_3OO^{\bullet}$ radical is exergonic with a negative ΔG value of -10.0 kcal mol^{-1}.

Additionally, the radical scavenging ability of falcarinol has been studied *via* another reactive radical such as $HO^{\bullet}$. H-atom abstraction at C3–H position and addition reactions at C4≡C5 triple bond that showed as the most feasible ones in the reaction with $CH_3OO^{\bullet}$ were taken into account. These reactions are chosen because they are shown as the most feasible ones in terms of energy. These reactions pass transition states, called TS-C3-absHO and TS-C4-addHO, at -5.7 and -5.3 kcal mol^{-1} lying under reactants that are followed by product complexes, namely PC-C3-absHO and PC-C4-addHO, at considerably negative energy of -54.7 and -42.9 kcal mol^{-1}, respectively. It is noted that these reactions are exergonic, showing negative ΔG values of -47.1 and -32.2 kcal mol^{-1}, in sequence (Table 4). In comparison with the reactions with $CH_3OO^{\bullet}$ radical, it is observed that the ones with $HO^{\bullet}$ are more feasible and higher exergonic.

3.2.2. Addition reaction at unsaturated bond positions. The addition reactions are set on the possible and less steric hindrance positions of unsaturated bonds. The PES of addition reactions between $CH_3OO^{\bullet}$ radical and falcarinol at C1, C4, C5, C6, C7 and C10 side is displayed in Fig. 2. The reactions generally start with the formation of reactants complexes lying

below reactants of −2.4, −1.1, −4.7, −2.0, −2.3 and −3.3 kcal mol^{-1} corresponding to addition at the C1, C4, C5, C6, C7 and C10 positions. Following this state, the reactions pass transition states (TS), namely TS-C1add, TS-C4add, TS-C5add, TS-C6add, TS-C7add and TS-C10add at the energy barriers of 10.1, 9.6, 15.5, 17.1, 9.6 and 9.3 kcal mol^{-1}, respectively, in which the C1–O, C4–O, C5–O, C6–O, C7–O and C10–O distances are 1.856, 1.918, 1.843, 1.839, 1.915 and 1.899 Å, in sequence. The product complexes (PC) are yielded by forming the C1–O, C4–O, C5–O, C6–O, C7–O and C10–O bonds of 1.443, 1.386, 1.408, 1.406, 1.387 and 1.455 Å, respectively. The relative energies of these states are 0.4, −9.9, 4.5, 5.0, −8.4 and 0.5 kcal mol^{-1}, respectively. All addition reactions showing positive ΔG values are determined to be endergonic (as shown in Table 2). It is clearly observed that the additions at C4 and C7 seem to be kinetically and thermodynamically more favorable, in which the reactions involve lower energy barriers than those for other addition reactions. For example, the energy barriers require for the addition at C4 and C7 are 10.7 and 11.9 kcal mol^{-1} compared to the values of 12.5, 20.2, 19.1 and 12.6 kcal mol^{-1} corresponding to the addition at C1, C5, C6 and C10, respectively.

Since α-vetivone appears as a promising antioxidant *via* HAT and SET-PT mechanism, attack of $CH_3OO^{\bullet}$ and $HO^{\bullet}$ radicals on this molecule was similarly investigated. The reactions were performed at easiest C8–H breaking bond and C9=C10 double bonds (as shown in Fig. 5). IRC plots for all transition states related to reaction of $CH_3OO^{\bullet}$ and $HO^{\bullet}$ radicals with α-vetivone are presented in Fig. S3 of ESI.†

Before attaining product complex (PC), all reactions firstly pass transition state (TS) with energy of 12.3, 9.3, −3.6 and −4.7 kcal mol^{-1} corresponding to TS-addCH_3OO, TS-absCH_3-OO, TS-absHO and TS-addHO, in turn (as seen in Fig. 6). The results underline that the H-atom abstractions by both radicals are more prominent than the addition ones. Indeed, PC-absCH_3OO and PC-absHO are found at −7.8 and −41.9 kcal mol^{-1} while PC-addCH_3OO and PC-addHO are determined at 0.8 and −25.3 kcal mol^{-1}, respectively (Fig. 6). As energy of product complex of the reaction with $HO^{\bullet}$ are much lower than the one with $CH_3OO^{\bullet}$ radical, the scavenging of $HO^{\bullet}$ is indicated to be more favorable. Moreover, the results show that the H-abstraction reaction with $CH_3OO^{\bullet}$ is slightly endergonic with low positive ΔG value of 1.5 kcal mol^{-1} (as shown in Table 4), while the addition one is more strongly endergonic with notably positive ΔG value of 18.0 kcal mol^{-1}. Oppositely, the reactions with $HO^{\bullet}$ are more exergonic with meaningfully negative ΔG values of −36.2 and −14.3 kcal mol^{-1} corresponding to H-abstraction and addition reactions, respectively (Table 4). This observation follows the same tendency as in the case of falcarinol. Note that the antioxidant molecules preferentially react with reactive $HO^{\bullet}$ radical.

3.2.3. Natural bond orbital (NBO) analysis. In order to understand the antioxidant mechanism, singly-occupied molecular orbital (SOMO) and atomic spin density (ASP) of the optimized transition states of the H-atom abstraction at C3–H and the addition reactions at different π-bonds along molecular chain of falcarinol by $CH_3OO^{\bullet}$ radical, as an example, were analyzed (as showed in Fig. 5).

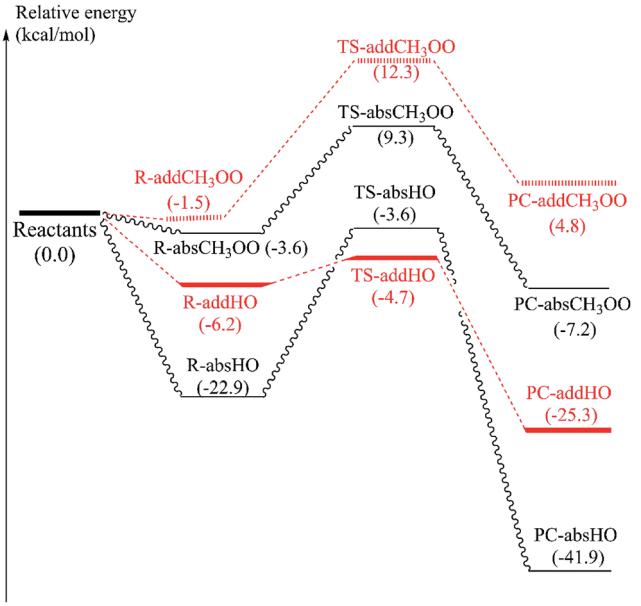

Fig. 6 PES at B3LYP/6-311G(d,p) level of theory of H-atom abstraction reaction at easiest C8–H breaking bond and addition reaction at C9 positions for α-vetivone and $CH_3OO^{\bullet}$ and $HO^{\bullet}$ radicals.

Concerning H-atom abstraction reaction at C3, it is widely accepted that there are two mechanisms which generate the same products as HAT: sequential electron proton transfer (SEPT) and proton coupled electron transfer (PCET). They correspond to single electron transfer followed by or occurred simultaneously with proton transfer, respectively.[39] In order to distinguish which kinds of mechanism falcarinol undergoes, natural bond population (NPA) charge, atomic spin density (ASP) and singly-occupied molecular orbitals (SOMO) analyses are systematically investigated for transition state of HAT reaction (Fig. 7A). As a result, the NPA charge indicates that O1-atom of the $CH_3OO^{\bullet}$ radical carries a negative charge, *i.e.* −0.3771*e*, while H3-atom which split from C3 atom on falcarinol, shows a positive value of 0.1712*e*. So the $CH_3OO^{\bullet}$ free radical possesses high nucleophile character which favors an attack to the H3–C3 electrophile active sites. As observed on ASP distribution in Fig. 7A, ASP distribution which consists in coefficient of the natural orbital carrying unpaired electron, of the transition state concentrates on two heavy atoms which undergo the H atom exchange, *i.e.* C3 and O1 atoms. This is corresponding to a HAT process.[40] Indeed, Mulliken APS analyses show that O and C3 atoms carry high positive spin density of 0.4366 and 0.2273, respectively, while APS of H atom is slightly negative, *i.e.* −0.0247. Furthermore, the SOMO has a significant atomic orbital density oriented along the transition vector, essentially localized on the C3···H3···O1 vector, with a node plane located at the migrating H3 transferring atom. The NBO analysis indicates that the third lone pair of electrons on O1 atom, LP(3)O1, is donated to an unoccupied σ* antibonding orbital on C3–H3, σ*(1)C3–H3, in the HAT process with stabilization energy equal to 44.2 kcal mol^{-1} in forming a new σ-bond O1–H3 on CH_3OOH (Table 5).

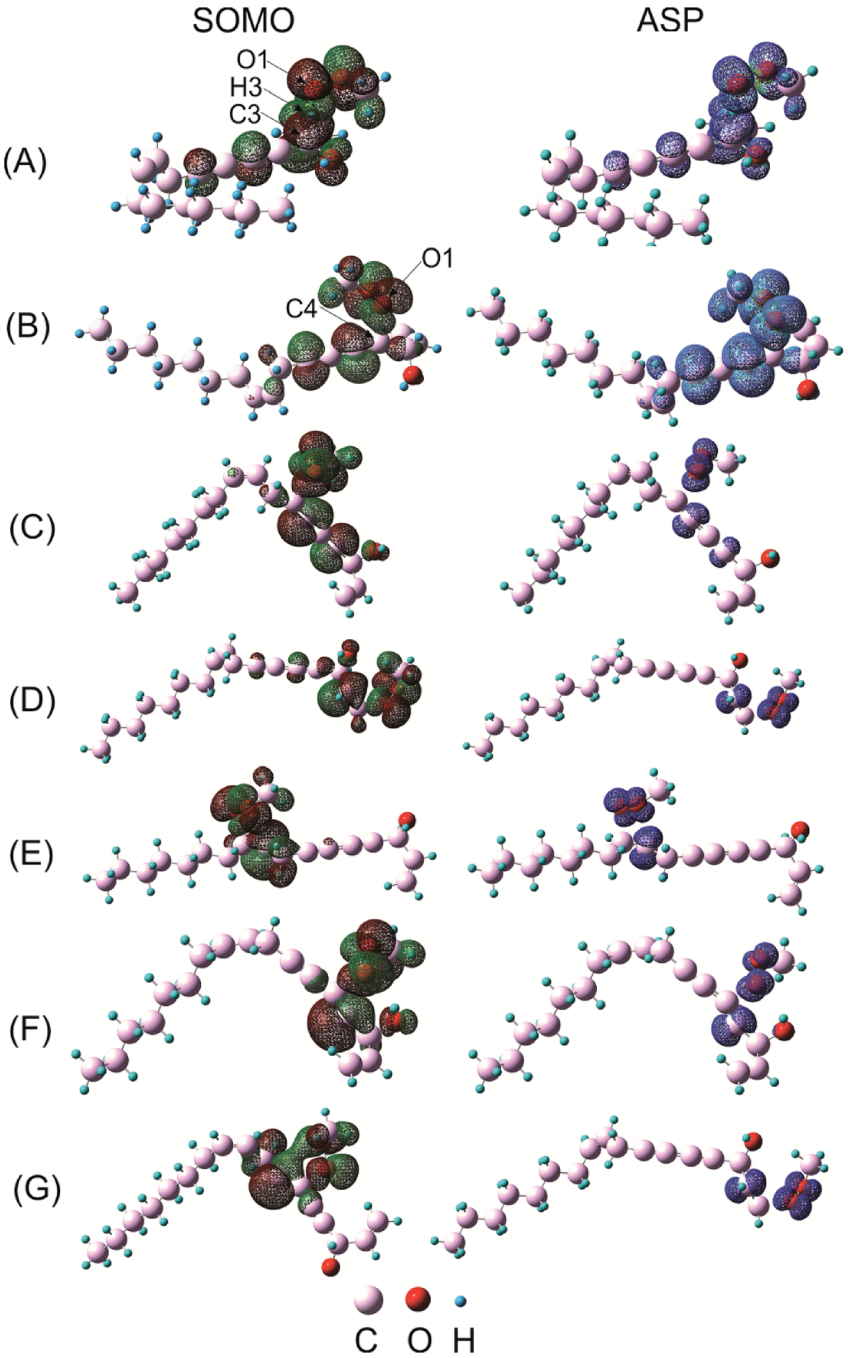

Fig. 7 SOMO densities surface and atomic spin density (ASP) of (A) H-abstraction at C3 and addition reactions at (B) C4; (C) C7; (D) C1; (E) C10; (F) C5and (G) C6 between $CH_3OO^{\bullet}$ radical and falcarinol. (Orbital density is visualized at isovalue of 0.02 and spin density is mapped from -5×10^{-4} to 5×10^{-4} at isovalue of 0.004).

For the radical addition reaction to C4≡C5 bond (Fig. 7B), the NPA charge calculation shows that O1-atom of the free radical carries high negative charge, *i.e.* −0.3639*e*, in acting as a nucleophile. Meanwhile, the C4 atom where the free radical attacks, carries small positive charge, *i.e.* 0.1411*e*, in showing as an electrophile. The Mulliken spin density distribution shows high spin density concentrated on O1 atom which has a tendency to approach to C4 carbon atom (Fig. 7B). Meanwhile, the SOMO shows that p orbital on O1-atom has high tendency to overlap with π-orbital on the C4≡C5 triple bond. The NBO analysis confirms that the third lone pair of electron on O1 atom, LP(3)O1 is transferred to the third unoccupied σ* antibonding orbital of the triple bond, σ*(3)C4–C5, with stabilization energy equal to 28.9 kcal mol^{-1}. This process tends to form σ-bond C4–O1, and results in loss of one π-bond between C4 and C5 atoms which changes it to a double bond. The observation for the other addition reactions is quite similar (Fig. 7C–G) (Table 5). The electron densities will then be shifted from

Table 5 Natural bond analysis of transition states of H-atom abstraction reactions and radical addition to π-bonds reactions[a]

	Donor NBO (i)	Acceptor NBO (j)	$E(2)$, kcal mol^{-1}
FALC–C3H + $CH_3OO^{\bullet}$	LP(3) O1	σ*(1) C1–H3	44.2
FALC–C10 + $CH_3OO^{\bullet}$	LP(3) O1	σ*(2) C9–C10	34.6
FALC–C7 + $CH_3OO^{\bullet}$	LP(3) O1	σ*(3) C6–C7	28.9
	π(3) C6–C7	σ*(2) C4–C5	16.8
	σ*(2) C6–C7	σ*(3) C4–C5	58.1
	σ*(3) C6–C7	σ*(2) C4–C5	56.2
FALC–C6 + $CH_3OO^{\bullet}$	LP(3) O1	σ*(2) C6–C7	40.1
	σ*(3) C6–C7	σ*(3) C4–C5	15.7
	σ*(2) C6–C7	σ*(2) C4–C5	13.1
FALC–C5 + $CH_3OO^{\bullet}$	LP(3) O1	σ*(2) C4–C5	38.6
FALC–C4 + $CH_3OO^{\bullet}$	LP(3) O1	σ*(3) C4–C5	28.9
	π(3) C4–C5	σ*(2) C6–C7	15.7
	σ*(2) C4–C5	σ*(3) C6–C7	59.5
	σ*(3) C4–C5	σ*(2) C6–C7	53.8
FALC–C1 + $CH_3OO^{\bullet}$	LP(3) O1	σ*(2) C1–C2	39.4

[a] π denotes π bonding orbital. σ* denotes sigma antibonding orbital. LP symbolizes a lone pair of electrons. LP(n) symbolizes the n^{th} lone pair of electrons.

bonding and antibonding orbitals of C4≡C5 bond like π(3) C4≡C5, σ*(2) C4–C5 and σ*(3) C4–C5 to the others vacant antibonding orbitals such as σ*(2) C6–C7, σ*(3) C6–C7 with the stabilization energy equal to 15.7, 59.5 and 53.8 kcal mol^{-1}, respectively. The observation for the other addition reactions is quite similar (Fig. 7C–G).

4. Conclusions

The thermochemical parameters of twenty-one oxygenated monoterpene and desquiterpene compounds extracted from *Cleistocalyx operculatus* have been studied in detail. Falcarinol is determined as the most effective antioxidant on the basis of both HAT and SPLET mechanisms. In fact, the BDE and PA in the gas phase of falcarinol are 66.5 kcal mol^{-1} and 341.3 kcal mol^{-1}. The effective property of falcarinol is a result of the presence of both OH group and unsaturated double/triple bonds in this molecule. Regarding the effect of solvent, it is observed that the hydrogen atom transfer is favorable in nonpolar environment while deprotonation process is supported by polar one where protons show higher solvation enthalpy. Calculated quantum chemical parameters underline that α-vetivone represent as the most reactive compounds with the chemical hardness of 4.02 eV and electrophilicity being 2.03 eV. This molecule also displays as one of the easiest electron removal with IE value of 8.06 eV.

From the potential energy surface (PES) point of view, the interaction between $CH_3OO^{\bullet}$ radical and falcarinol were clarified. The H-abstraction reaction at C3–H position is determined as the most favored with the energy barriers of −18.7 kcal mol^{-1}. Among the addition reactions, the ones at C4 position of C4≡C5 and C7 of C6≡C7 triple bonds are the most favored with the energy barriers of −9.9 and −8.4 kcal mol^{-1}, respectively. And it is shown that the H-abstraction reaction is exergonic with a negative ΔG value of −10.0 kcal mol^{-1}, while all addition reactions are endergonic with positive ΔG value from 1.7 to 16.6 kcal mol^{-1}.

Interaction between falcarinol and reactive $HO^{\bullet}$ radical was also considered. The PES for H-atom abstraction reaction at the easiest C3–H breaking bond and the addition reaction at C4 position were investigated. In comparing to the reactions with $CH_3OO^{\bullet}$, it is observed that falcarinol reacts more strongly with $HO^{\bullet}$ radical with significantly lower ΔH and ΔG values, *i.e.* −54.7 and −47.1 kcal mol^{-1}, respectively for H-abstraction reaction, and −42.9 and −32.2 kcal mol^{-1}, respectively for addition one.

Singly-occupied molecular orbital (SOMO), natural population atomic (NPA) charge, atomic spin density (ASP) and natural bond orbital (NBO) analysis of the optimized transition states of the reactions between falcarinol and $CH_3OO^{\bullet}$ radical have been performed, as an example, to clarify the mechanism of these reactions. The mechanism is determined by the transfer of the third lone pair of electrons on O1-atom of $CH_3OO^{\bullet}$ radical to an unoccupied σ* antibonding orbital on C3–H3, and on the triple C4≡C5, C6≡C7 bonds.

In the case of α-vetivone, attack of $CH_3OO^{\bullet}$ and $HO^{\bullet}$ at easiest C8–H breaking bond and at C9=C10 double bonds was similarly studied. The results show that the H-atom abstraction reactions by both radicals are more prominent than the addition ones. Indeed, the energy of product complex for H-abstraction by $CH_3OO^{\bullet}$ and $HO^{\bullet}$ radicals are found −7.2 and −41.9 kcal mol^{-1} while the ones of addition reaction are determined at 4.8 and −25.3 kcal mol^{-1}, respectively. The reactions with $HO^{\bullet}$ are more exergonic than the ones with $CH_3OO^{\bullet}$ radical with meaningfully negative ΔG values of −36.2 and −14.3 kcal mol^{-1} corresponding to H-abstraction and addition reactions, respectively.

According to the results obtained for falcarinol, it could conclude that the antioxidant molecules preferably react with reactive $HO^{\bullet}$ radical.

Conflicts of interest

There are no conflicts to declare.

Acknowledgements

This research is funded by Vietnam National Foundation for Science and Technology Development (NAFOSTED) under grant number 104.06-2015.09.

References

1 C. Cabrera, R. Gimenez and M. C. Lopez, *J. Agric. Food Chem.*, 2003, **51**, 4427–4435.
2 G. Singh, S. Maurya, C. Catalan and M. P. De Lampasona, *J. Agric. Food Chem.*, 2004, **52**, 3292–3296.
3 A. I. Hussain, F. Anwar, S. T. Hussain Sherazi and R. Przybylski, *Food Chem.*, 2008, **108**, 986–995.
4 K. A. Youdim, S. G. Deans and H. J. Finlayson, *J. Essent. Oil Res.*, 2002, **14**, 210–215.

5 M. Hyldgaard, T. Mygind and R. L. Meyer, *Front. Microbiol.*, 2012, **3**, 12.
6 B. Bozin, N. Mimica-Dukic, N. Simin and G. Anackov, *J. Agric. Food Chem.*, 2006, **54**, 1822–1828.
7 V. R. Preedy, *Essential Oils in Food Preservation, Flavor and Safety*, Academic Press, 2015.
8 H. Robert, in *Handbook of Essential Oils*, CRC Press, 2015, pp. 381–431.
9 L.-B. Maria, in *Handbook of Essential Oils*, CRC Press, 2015, pp. 619–653.
10 K. H. Baser and B. Gerhard, in *Handbook of Essential Oils*, CRC Press, 2015, pp. 1–3.
11 M. K. Fasseas, K. C. Mountzouris, P. A. Tarantilis, M. Polissiou and G. Zervas, *Food Chem.*, 2008, **106**, 1188–1194.
12 S. Chatterjee, Z. Niaz, S. Gautam, S. Adhikari, P. S. Variyar and A. Sharma, *Food Chem.*, 2007, **101**, 515–523.
13 H.-Y. Chen, Y.-C. Lin and C.-L. Hsieh, *Food Chem.*, 2007, **104**, 1418–1424.
14 C. Turek and F. C. Stintzing, *Compr. Rev. Food Sci. Food Saf.*, 2013, **12**, 40–53.
15 J. G. Lopez-Reyes, D. Spadaro, A. Prelle, A. Garibaldi and M. L. Gullino, *J. Food Prot.*, 2013, **76**, 631–639.
16 R. Lawrence and K. Lawrence, *Asian Pac. J. Trop. Biomed.*, 2011, **1**, S51–S54.
17 B. Bozin, N. Mimica-Dukic, N. Simin and G. Anackov, *J. Agric. Food Chem.*, 2006, **54**, 1822–1828.
18 N. T. Dung, J. M. Kim and S. C. Kang, *Food Chem. Toxicol.*, 2008, **46**, 3632–3639.
19 T. C. Ngo, D. Q. Dao, N. M. Thong and P. C. Nam, *RSC Adv.*, 2016, **6**, 30824–30834.
20 S. Purup, E. Larsen and L. P. Christensen, *J. Agric. Food Chem.*, 2009, **57**, 8290–8296.
21 J. F. Young, L. P. Christensen, P. K. Theil and N. Oksbjerg, *Dose-Response*, 2008, **6**, 239–251.
22 I.-Y. Choi, J. H. Lim, S. Hwang, J.-C. Lee, G.-S. Cho and W.-K. Kim, *Free Radical Res.*, 2010, **44**, 541–551.
23 P. C. Lars, *Recent Pat. Food, Nutr. Agric.*, 2011, **3**, 64–77.
24 H.-J. Kim, F. Chen, X. Wang, H. Y. Chung and Z. Jin, *J. Agric. Food Chem.*, 2005, **53**, 7691–7695.
25 M. J. Frisch, G. W. Trucks, H. B. Schlegel, G. E. Scuseria, M. A. Robb, J. R. Cheeseman, G. Scalmani, V. Barone, B. Mennucci, G. A. Petersson, H. Nakatsuji, M. Caricato, X. Li, H. P. Hratchian, A. F. Izmaylov, J. Bloino, G. Zheng, J. L. Sonnenberg, M. Hada, M. Ehara, K. Toyota, R. Fukuda, J. Hasegawa, M. Ishida, T. Nakajima, Y. Honda, O. Kitao, H. Nakai, T. Vreven, J. A. Montgomery Jr, J. E. Peralta, F. Ogliaro, M. Bearpark, J. J. Heyd, E. Brothers, K. N. Kudin, V. N. Staroverov, T. Keith, R. Kobayashi, J. Normand, K. Raghavachari, A. Rendell, J. C. Burant, S. S. Iyengar, J. Tomasi, M. Cossi, N. Rega, J. M. Millam, M. Klene, J. E. Knox, J. B. Cross, V. Bakken, C. Adamo, J. Jaramillo, R. Gomperts, R. E. Stratmann, O. Yazyev, A. J. Austin, R. Cammi, C. Pomelli, J. W. Ochterski, R. L. Martin, K. Morokuma, V. G. Zakrzewski, G. A. Voth, P. Salvador, J. J. Dannenberg, S. Dapprich, A. D. Daniels, O. Farkas, J. B. Foresman, J. V. Ortiz, J. Cioslowski and D. J. Fox, *Gaussian 09, Revision E.01*, Gaussian, Inc., Wallingford CT, 2013.
26 N. M. Thong, D. T. Quang, N. H. T. Bui, D. Q. Dao and P. C. Nam, *Chem. Phys. Lett.*, 2015, **625**, 30–35.
27 J. E. Bartmess, *J. Phys. Chem.*, 1994, **98**, 6420–6424.
28 K. K. Irikura, R. D. Johnson and R. N. Kacker, *J. Phys. Chem. A*, 2005, **109**, 8430–8437.
29 E. Cancès, B. Mennucci and J. Tomasi, *J. Chem. Phys.*, 1997, **107**, 3032–3041.
30 J. Tomasi, B. Mennucci and E. Cancès, *J. Mol. Struct.: THEOCHEM*, 1999, **464**, 211–226.
31 I. B. Obot, D. D. Macdonald and Z. M. Gasem, *Corros. Sci.*, 2015, **99**, 1–30.
32 H. Chermette, *J. Comput. Chem.*, 1999, **20**, 129–154.
33 R. P. Iczkowski and J. L. Margrave, *J. Am. Chem. Soc.*, 1961, **83**, 3547–3551.
34 R. G. Parr, L. v. Szentpály and S. Liu, *J. Am. Chem. Soc.*, 1999, **121**, 1922–1924.
35 G. Wang, Y. Xue, L. An, Y. Zheng, Y. Dou, L. Zhang and Y. Liu, *Food Chem.*, 2015, **171**, 89–97.
36 M. Li, W. Liu, C. Peng, Q. Ren, W. Lu and W. Deng, *Int. J. Quantum Chem.*, 2013, **113**, 966–974.
37 A. Pérez-González and A. Galano, *Int. J. Quantum Chem.*, 2012, **112**, 3441–3448.
38 M. C. Foti, *J. Agric. Food Chem.*, 2015, **63**, 8765–8776.
39 S. Olivella, J. M. Anglada, A. Solé and J. M. Bofill, *Chem.–Eur. J.*, 2004, **10**, 3404–3410.
40 J. M. Mayer, D. A. Hrovat, J. L. Thomas and W. T. Borden, *J. Am. Chem. Soc.*, 2002, **124**, 11142–11147.

